ARTICLE IN PRESS

Optics Communications ▮ (▮▮▮▮) ▮▮▮–▮▮▮

Contents lists available at ScienceDirect

Optics Communications

journal homepage: www.elsevier.com/locate/optcom

Optical contrast for identifying the thickness of two-dimensional materials

Dan Bing [a,*], Yingying Wang [b], Jing Bai [a], Ruxia Du [a], Guoqing Wu [a], Liyan Liu [c]

[a] Department of Basic Teaching, Nanjing Tech University Pujiang Institute, Nanjing 211134, China
[b] Department of Optoelectronic Science, Harbin Institute of Technology at Weihai, Weihai 264209, China
[c] The 723 Institute of CSIC, Yangzhou 225001, China

ARTICLE INFO

Keywords:
Two dimensional materials
Optical contrast
Graphene
Thickness identification

ABSTRACT

One of the most intriguing properties of two-dimensional (2D) materials is their thickness dependent properties. A quick and precise technique to identify the layer number of 2D materials is therefore highly desirable. In this review, we will introduce the basic principle of using optical contrast to determine the thickness of 2D material and also its advantage as compared to other modern techniques. Different 2D materials, including graphene, graphene oxide, transitional metal dichalcogenides, black phosphorus, boron nitride, have been used as examples to demonstrate the capability of optical contrast methods. A simple and more efficient optical contrast image technique is also emphasized, which is suitable for quick and large-scale thickness identification. We have also discussed the factors that could affect the experimental results of optical contrast, including incident light angle, anisotropic nature of materials, and also the twisted angle between 2D layers. Finally, we give perspectives on future development of optical contrast methods for the study and application of 2D materials.

1. Introduction

Two dimensional (2D) materials have attracted great attentions for the past decade due to its unique properties and great potential for applications. As an example, graphene, a single layer of carbon atoms arranged with honeycomb lattices, has ultrahigh mobility, superior mechanical and thermal properties, while at the same time is transparent but conductive, which make it promising candidate for electronics and optoelectronics [1,2]. After the discovery of graphene in 2004, different kinds of 2D materials have been explored, including layered transitional metal dichalcogenides (TMDs) [3,4], black phosphorus (BP) [5], boron nitride (BN) [6], antimonene [7], silicene [8], germanene [9]. These materials cover a broad range of electronic bandgap, from 0–~4 eV, which are suitable for different electronic devices. For example, TMDs are great for logic devices with high on/off ratio [3], graphene and BP is ideal for infrared photodetectors [10], BN is suitable as insulator buffer layers or substrates [11,12].

One of the most interesting behaviors of 2D materials is that their properties are strongly dependent on thickness or layer numbers. For example, single layer graphene has linear dispersive electronic band structure and nearly zero electron mass, while bi- and multi-layer graphene possesses massive Dirac fermions and its band structure can be tuned by perpendicular electric field [13]. On the other hand, most of the TMDs materials, including MoS_2 and WS_2, are direct bandgap semiconductors in monolayer, and becoming indirect bandgap materials when their thicknesses are more than two layers [14]. The bandgap of BP can be tuned from 0.3 eV to ~1.8 eV from bulk to single layer [15]. Therefore, it is of great importance to identify the thickness of 2D materials unambiguously and efficiently.

Modern techniques have been adopted to characterize the thickness of 2D materials, including transmission electron microscope (TEM) [16], atomic force microscope (AFM) [17], low energy electron microscopy (LEEM) [18], scanning tunneling microscope (STM) [19] and so on. Although these techniques have very high spatial resolution and can even resolve single atoms, they suffer from low throughput or complicate sample preparation. Optical techniques have the advantage of non-contact, quick and capable for large-scale investigation, which are ideal for the thickness identification of 2D materials. For example, Raman spectroscopy has been widely used to study graphitic materials, and can provide information on layer numbers, strain, doping, defects, and electronic bandstructures of graphene [20]. Photoluminescence (PL) spectroscopy is also frequently used to study the photo emission of 2D semiconductors with different thicknesses [21,22]. For example, the PL intensity of monolayer TMDs is 1–2 orders higher than that of multilayers, due to the difference of direct and indirect bandgap structure [14]. On the other hand, the PL emission can vary from

* Corresponding author.
E-mail address: bingdan81@hotmail.com (D. Bing).

http://dx.doi.org/10.1016/j.optcom.2017.06.012
Received 25 March 2017; Received in revised form 23 May 2017; Accepted 2 June 2017
Available online xxxx
0030-4018/

Please cite this article in press as: D. Bing, et al., Optical contrast for identifying the thickness of two-dimensional materials, Optics Communications (2017), http://dx.doi.org/10.1016/j.optcom.2017.06.012.

~700 nm of single layer phosphorene to ~2 μm for samples of ~5 layers [15]. Second harmonic generation signals of TMDs are distinct for samples with odd and even layers [23]. However, in term of thickness characterization, Raman spectroscopy is normally used for graphene layer number determination of 1–4 layers [24], while PL spectroscopy can be used to identifying some of the direct bandgap semiconductors. On the other hand, optical contrast spectroscopy and images are the most commonly used tools for thickness identification of 2D materials [21,24–31]. They are easily operated, fast, and can be adapted to almost all the 2D materials, including graphene, graphene oxide (GO), TMDs, BP and BN. Different parameters that could affect the optical contrast of 2D materials have been reported and discussed extensively, e.g. refractive index of the multi-layer substrate and top deposition layer, incident angles, twist angles between 2D layers [32–37]. Most importantly, the optical contrast does not require expensive equipment and is ready for large-scale investigation.

In this review, we will discuss the recent progress on optical contrast of 2D materials. In Section 2, the basic working principle of optical contrast is presented. In Section 3, the use of optical contrast to determine the thickness of different 2D materials will be given, including graphene, GO, TMDs, BP and other 2D materials. In Section 4, an optical contrast image technique which is favored for large-scale thickness identification will be discussed. In Section 5, different factors that would affect the optical contrast of 2D materials will be discussed, including the incident angle of light, anisotropic natures of materials and twist angle between 2D layers. Finally, we discuss the perspective and challenges of optical contrast studies.

2. Working principle of optical contrast spectroscopy

The basic principle of using optical contrast to determine the thickness of 2D materials is shown in Fig. 1. When a 2D material is deposited on a substrate, due to the absorption of the material or change of the length of optical path if there is a multilayer structure, the intensity of reflection light from the sample would be different substrate. As an example, when a single graphene sheet is deposited on 285 nm SiO_2/Si substrate, it looks darker compared to substrate, as shown in Fig. 1(a), which means the light reflected from graphene is weaker compared to SiO_2/Si substrate. This can be easily understood by Fresnel law of multilayer interference as shown in Fig. 1(b). When a beam of polarized light (s-wave or p-wave) is incident at an interface with incident angle θ_1, for example, air/SiO_2 interface, a portion of the beam is reflected from the interface and the rest is transmitted, thus, an infinite number of optical paths are possible as schematically shown in Fig. 1(b). Take air/SiO_2/Si system for example, the total reflected amplitude r_0 is governed by Eq. (1) [24],

$$r_0 = \frac{r_{02} + r_{23} \cdot e^{-2i\phi_2}}{1 + r_{02} \cdot r_{23} \cdot e^{-2i\phi_2}}. \tag{1}$$

Similarly, for air/graphene/SiO_2/Si system, the total reflected amplitude r_1 can be calculated by Eq. (2),

$$r_1 = \frac{r_{01} + r_{01}r_{12}r_{23}e^{-2i\phi_2} + r_{12}e^{-2i\phi_1} + r_{23}e^{-2i(\phi_1+\phi_2)}}{1 + r_{12}r_{23}e^{-2i\phi_2} + r_{01}r_{12}e^{-2i\phi_1} + r_{01}r_{23}e^{-2i(\phi_1+\phi_2)}}. \tag{2}$$

Here, r_{ij} is reflection coefficient at the layer i/layer j interface. At normal incident, r_{ij} can be calculated by $r_{ij} = \frac{\tilde{n}_i - \tilde{n}_j}{\tilde{n}_i + \tilde{n}_j}$. $\tilde{n}_i$ ($\tilde{n}_j$) is the complex refractive index of layer i (layer j). At oblique incident, in the calculation of reflection coefficient, for s-polarized light, $\tilde{n}_i$ should be replaced by $\tilde{n}_i \cos\theta_i$. While for p-polarized light, $\tilde{n}_i$ should be replaced by $\tilde{n}_i / \cos\theta_i$. $\phi_2 = \frac{2\pi \cdot n_2 \cdot d_2 \cdot \cos\theta_2'}{\lambda}$ and $\phi_1 = \frac{2\pi \cdot \tilde{n}_1 \cdot d_1 \cdot \cos\theta_2}{\lambda}$ are individual phase differences when light passes through SiO_2 layer and graphene layer. $\theta_2'(\theta_2)$ is the refraction angle in SiO_2 (graphene) layer. $n_2(\tilde{n}_1)$ is the refractive index of SiO_2 (graphene) layer. d_2 (d_1) is the thickness of the SiO_2 (graphene) layer. λ is wavelength. The reflection spectrum from air/(SiO_2 on Si), $R_0(\lambda)$ can be calculated by

$$R_0(\lambda) = |r_0|^2. \tag{3}$$

The reflection spectrum from air/graphene/SiO_2/Si system, $R_1(\lambda)$ can be calculated by

$$R_1(\lambda) = |r_1|^2. \tag{4}$$

For unpolarized light, one can take an average of the contribution from both s-wave and p-wave. Furthermore, including effect of numerical aperture (NA) of the microscope objective in the calculation of contrast, the reflection spectrum $R_{0,1}(\lambda)$ should be modified by numerical integration of the reflectance values (computed for various angles of incidence) over the solid angle determined by each NA

$$R_{0,1} = 2\pi \int_0^{\theta_m} R_{0,1}(\theta) W(\theta) \sin\theta d\theta \tag{5}$$

where $\theta_m = \arcsin(NA)$ and $W(\theta)$ is a weight function that indicates the angular distribution of the collected light [38,39], e.g., uniform distribution $W(\theta) = \text{const}$, Gaussian distribution $W(\theta) = e^{-\frac{2\sin^2\theta}{\sin^2\theta_m}}$ and so on.

The interference effect is strongly dependent on the wavelength of incident light. Therefore, the intensity of reflection light is also wavelength dependent, as does the optical contrast. This can be clearly shown in the reflection spectra in Fig. 1(c). The reflection spectrum from graphene R_1 is weaker than that from pure SiO_2/Si substrate R_0 in the wavelength range of 500–650 nm, corresponding to the wavelength where interference effect is strongest on 285 nm/Si substrate. The optical contrast spectrum between sample and substrate can be then be derived by following equations: $C(\lambda) = (R_0(\lambda) - R_1(\lambda))/R_0(\lambda)$. Here, R_0–R_1 is used because most of the 2D materials behavior darker as compared to the substrate on multilayer substrate, and this will make the contrast value positive. The contrast spectrum of single layer graphene on 285 nm SiO_2/Si is shown in Fig. 1(d) [24], which has a peak centered at ~560 nm, and has a maximum value of ~0.1 (10%). This contrast peak is the reason why single layer graphene is visible and can be experimental exfoliated and located. There are two origins of such a high contrast of graphene on this specific substrate. Firstly, graphene has a universal optical absorption in visible range, and it can absorb ~2.3% of the incident light even for a monolayer layer. Secondly but importantly, the interference effect from the SiO_2/Si multilayer structure would strongly enhance the absorption of light. On the other hand, the optical contrast of single layer graphene on glass is much weaker (<5%) and can barely be seen, because there are no interference effect and the contrast comes purely from the absorption of graphene [40]. If a single layer graphene is deposited on Si or GaAs substrate [41], the optical contrast is even weaker, and it is not possible to be located by a common microscope or human eye. Methods for improving the optical contrast of graphene on insulating or semiconducting substrates will be discussed in the later section.

3. Optical contrast for identifying the thicknesses of 2D materials

It has been demonstrated above that the optical contrast value of 2D materials is related to substrate, incident wavelength, and most importantly, the thickness of two dimensional materials. Following, we will introduce the identification of thickness of different types of 2D materials by contrast spectroscopy, e.g. graphene, GO, TMDs, BP and BN.

3.1. Graphene

Fig. 2(a) shows the optical images as well as the corresponding contrast spectra of graphene layers with different thicknesses on 285 nm SiO_2/Si substrate [24]. It can be clearly seen that the intensity of contrast peak at ~550 nm increases gradually with the increase of thickness up to 10 layers. The highest contrast values are ~0.09, 0.175, 0.255, and 0.33 for 1–4 layers, respectively. The contrast value decreases for graphene layers >10 and finally negative contrast appears for samples

Please cite this article in press as: D. Bing, et al., Optical contrast for identifying the thickness of two-dimensional materials, Optics Communications (2017), http://dx.doi.org/10.1016/j.optcom.2017.06.012.

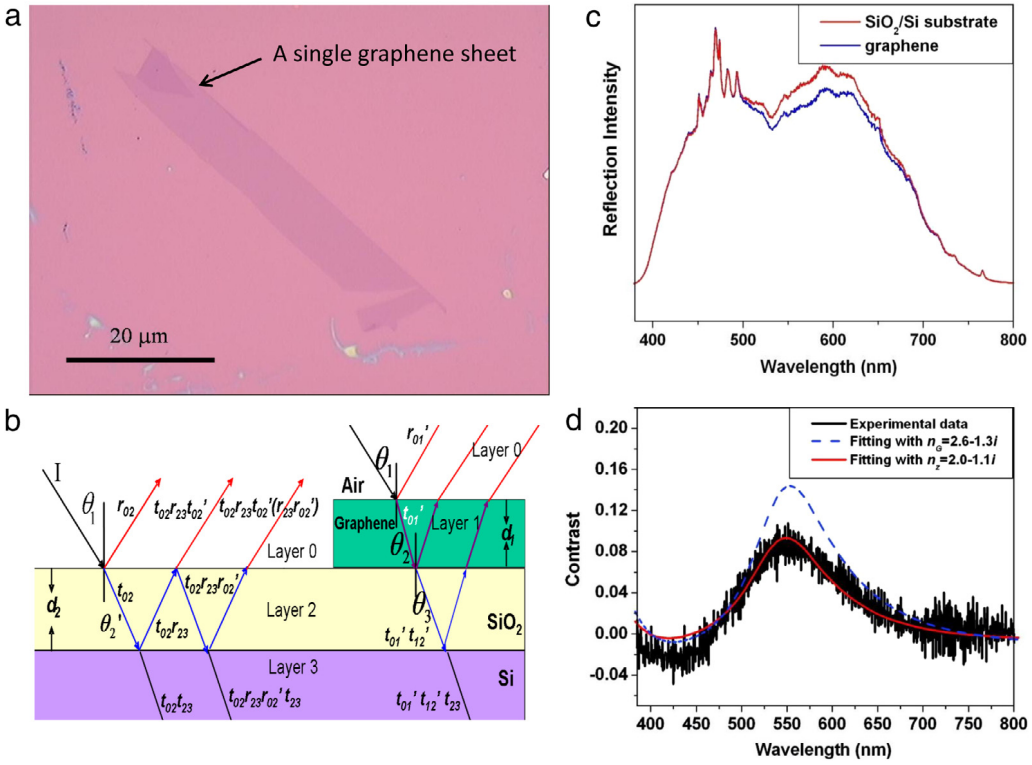

Fig. 1. Basic principle of optical contrast method. (a) Optical image of a single graphene sheet deposited on 285 nm SiO_2/Si substrate. (b) Schematic of multiple reflection and interference of graphene on SiO_2/Si substrate. (c) Reflection spectra of white light from SiO_2/Si substrate and graphene. (d) Contrast spectra of single layer graphene on 285 nm SiO_2/Si substrate [24].

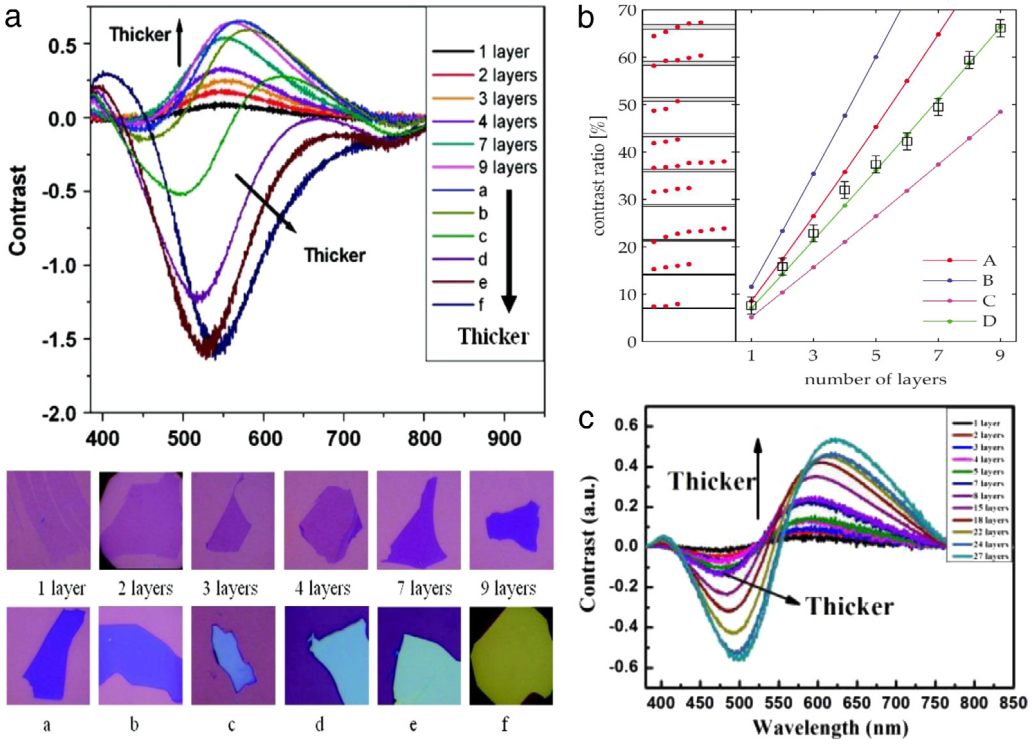

Fig. 2. Identify the thickness of graphene and GO using optical contrast. (a) Optical images and contrast spectra of graphene layers with different thicknesses on 285 nm SiO_2/Si substrate [24]. (b) Measured and theoretical calculated optical contrast of graphene flakes of 1–9 layers on glass substrate [40]. (c) Contrast spectra of GO with thickness up to 8 layers on 300 nm SiO_2/Si substrate [26].

which are so thick that the reflection from sample becomes dominant. A correlation between graphene layer numbers and contrast peak values for ≤9 layers have been given which is very useful and accurate for determining its thickness [24]. The optical contrast of graphene on SiO_2/Si substrate with different thickness of SiO_2 has also been studied and it shows that the values can be much different; with 90 nm SiO_2 gives the maximum contrast [42]. Therefore, it is very important to measure the thickness of dielectric materials before directly using the

Please cite this article in press as: D. Bing, et al., Optical contrast for identifying the thickness of two-dimensional materials, Optics Communications (2017), http://dx.doi.org/10.1016/j.optcom.2017.06.012.

contrast value to determine the thickness of graphene. The safe way would be make a calibration of the system by comparing the results with other techniques, e.g. Raman spectroscopy is a very reliable method to determine single layer graphene and the corresponding sample can be used for reference [20].

Different from SiO_2/Si substrate which has a strong interference effect, graphene on transparent substrate, e.g. glass, or other insulating materials, CaF_2, Al_2O_3 [43], can also be identified, but with much weaker contrast. However, the advantage is that the contrast values increase almost linearly with the thickness of graphene for 1–9 layers (Fig. 2(b)) [40]. This is because optical contrast mostly comes from the absorption of graphene layers and such values are solely determined by the thickness of graphene. It is even demonstrated that the linear regime can be extended to more than 100 layers [44]. The contrast values finally decrease due the interference effect of graphene layers itself when its thickness is comparable to the wavelength of the incident light. The ultimate example would be suspended graphene, whose contrast is 2.3% compared to air and increase almost linearly with the increase of graphene thickness [45].

The contrast of graphene on different substrate can be greatly enhanced by different routes. The most straightforward way would be designing a proper multilayer substrate. The dielectric 2D film on a multilayer substrate introduces a perturbation of the reflection of the substrate r. Therefore, by choosing an appropriate r, the perturbation, that is the optical contrast, could be maximized [46]. Results have shown that by using Al_2O_3/Si instead of SiO_2/Si, the optical contrast and the visibility of graphene could be greatly enhanced. Moreover, the Al_2O_3 substrate is better for electrical devices as compared to SiO_2 because the limited number of charged impurities [47]. The contrast of graphene on glass substrate is much weaker compared to multilayer substrate. Researchers found that by covering graphene with an immersion liquid with a refractive index that is close to that of the glass substrate, the optical contrast can be enhanced by a factor of 4 [48]. The contrasts of graphene on pure metal/semiconductor/insulator, e.g. Si, GaAs, are extremely weak and cannot even be resolved by human eyes. However, if an additional layer of PMMA or other resist layer is deposited on top of graphene/Si or graphene/GaAs, the optical contrast of single layer graphene could be enhanced to ~2.5%, which is enough for locating the sample. Namely, by coating optimum thickness of PMMA on graphene, it can be visualized on most of the materials [49]. It should be noted that the above routes for enhance the optical contrast of graphene are universal and could also be adapted to other 2D materials as discussed below.

3.2. Graphene oxide

GO is another member of graphene like materials, which is promising for application on energy storage, flexible transparent conductive film, and composite materials [50–52]. The properties of GO differ greatly from that of graphene since many oxygen-containing functional groups located either on the basal plane or at the edges [53]. The ability to reduce and even spatially control these oxygen groups in GO structures provides opportunities for tailoring its physical and chemical properties for various applications [54]. GO is normally insulating if the oxidation degree is high, and the bandgap could be more than 3 eV. Therefore, GO is almost transparent in visible region, and it is very difficult to identify monolayer GO by optical methods. GO can be reduced to remove the oxygen functional groups, either by chemical or thermal reduction [54], so that the properties of graphene could be partially recovered. Results have shown that the electrical conductivity as well as the optical absorption would be gradually enhanced with the increase of reduction degree [25].

A fluorescence quenching microscopy has been used to visualize GO by the strong quenching effect of GO upon its contact with fluorescence molecules, where charge transfer between the two objects play a most important role [55]. However, such method cannot be used to identify the thickness of GO, because the charge transfer effect or quenching efficiency is so strong for monolayer GO, and there is no difference for GO with different thicknesses. White light contrast spectroscopy has been used to evaluated the thickness of GO (Fig. 2(c)), and it is found that the contrast value of monolayer GO on 300 nm SiO_2/Si substrate is only 0.035, and increases almost linearly with the increase of thickness (up to 8 layers) [26]. It should be noted that if GO is totally insulating, it should be zero opacity. The contrast value could be even lower since in this case the contrast is caused by extra interference path due to the presence of a transparent sample on SiO_2/Si substrate only. While in the real case, the GO sample is difficult to be 100% oxidized and water or other molecule attached on GO sheets could also help on the absorption of light. As mentioned above, the properties of GO can be changed with the reduction process and the electrical conductivity as well as refractive index of GO can approach to that of graphene. Results have shown that the optical contrast of graphene oxide can be significantly different from GO, especially in the wavelength where interference effect takes parts [25].

3.3. TMDs

TMDs are new members of 2D materials, which have attracted great attentions due to their semiconducting properties as well as layer dependent electronic properties [3,4,56]. Recently, the valley dependent optical and electrical properties of TMDs have also been discovered, which ensures great potentials in electronic devices with new concept [57,58]. One of the most unique properties of most TMDs is the indirect to direct bandgap transition when the thickness is thinning down to monolayer. Hence, the identification of thickness of TMDs by optical methods was firstly realized by using PL spectroscopy [14]. The PL intensity of monolayer TMDs is much stronger than that of multilayers (Fig. 3(a)) [21], and the difference could be 1–2 orders. However, the PL intensity of monolayer TMDs is strongly influenced by different factors, e.g. doping, strain and defects. The n or p type doping would introduce a transition from neutral exciton to trion [4], and defects would induce bound exciton and strongly degrade the PL intensities [59]. While sometimes, the defect engineering could also form localized exciton and dramatically enhance the PL intensity [60]. Therefore, it is not accurate to use PL spectroscopy to determine the thickness of TMDs, especially for multilayer samples. On the other hand, Raman spectra have shown difference on TMDs with different thickness [61]. Take MoS_2 as an example, the frequency difference of two distinct Raman features, E_{2g} and A_{1g}, increase gradually with the increase of thickness (Fig. 3(b)), ~19 cm^{-1} for 1 layer and 20.5 cm^{-1} for 2 layers [21]. Contrast spectroscopy provides another route to verify the thickness of TMDs. The theoretical calculated optical contrast of MoS_2 with different thicknesses on quartz substrate is shown in Fig. 3(c) [62]. It can be seen that there are several optical contrast peaks, which corresponding to the peaks of real and imaginary part of the complex refractive index of MoS_2. The 620 nm and 680 nm peaks are corresponding to the absorption of A and B excitons [21]. By integrating the wavelength of 400–750 nm of the contrast spectra, one can obtain the theoretical optical contrast of MoS_2 on quartz substrate and the results with experimental contrasts are shown in Fig. 3(d) [62]. It can be seen that there are excellent match between theory and experiments and the optical contrast increases almost linearly with the thickness of MoS_2 (~0.7781 for 1 layer). If the MoS_2 samples are deposited on SiO_2/Si substrate, multilayer interference effects should be considered, and Fig. 3(e) shows the optical contrasts of MoS_2 with different thicknesses on 90 and 290 nm SiO_2/Si substrates (It should be noted that $C = (I_{flake} - I_{sub})/(I_{flake} + I_{sub})$ is using to obtain the contrast) [63]. As can be seen, the optical contrasts are negative for thin MoS_2 on 90 nm SiO_2/Si substrates for different incident wavelength, which means samples appear dark on substrate. When the flakes become thick, the reflection from MoS_2 increases and finally the contrasts are positive, which means the samples appear bright. The optical contrast of TMDs on SiO_2/Si substrate is strongly dependent on the thickness of SiO_2, with 90 and 300 nm substrates giving maximum contrast value, which is about twice as that of graphene on same substrate [27].

Please cite this article in press as: D. Bing, et al., Optical contrast for identifying the thickness of two-dimensional materials, Optics Communications (2017), http://dx.doi.org/10.1016/j.optcom.2017.06.012.

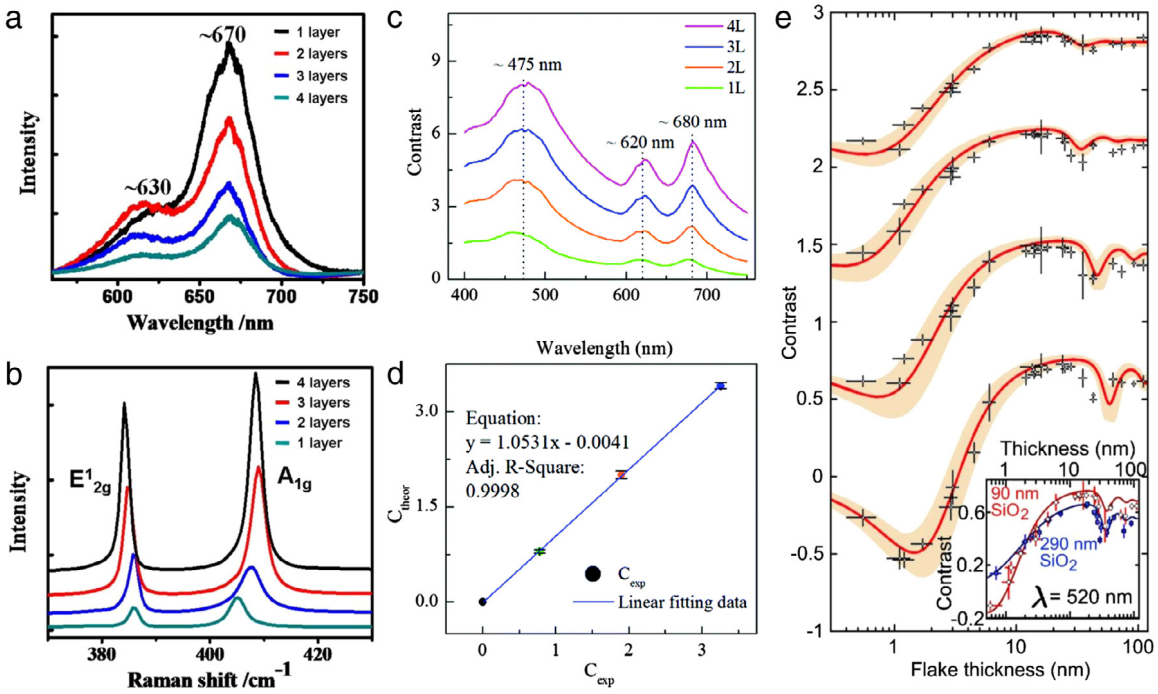

Fig. 3. The optical contrast of TMDs. PL (a) as well as Raman (b) spectra of MoS_2 of 1–4 layers [21]. (c) The theoretical calculated optical contrast of MoS_2 with different thicknesses on quartz substrate [62]. (d) The theoretical and experimental averaged optical contrast values of MoS_2 on quartz substrate in the wavelength range of 400–750 nm [62]. (e) The optical contrasts of MoS_2 with different thicknesses on 90 and 290 nm SiO_2/Si substrates [63].

3.4. BP and other 2D materials

In addition to graphene, there are also other 2D layered materials with single elements, e.g. BP, silicene, germanene and antimonene. These 2D materials are semiconducting and predicted to have ultrahigh electrical mobility and current on/off ratio. Taking BP as an example, it bridges the gap between graphene (zero-bandgap) and TMDs with bandgap in the visible regime. The hole mobility has been demonstrated to be ~1000 cm^2/Vs and with a on/off ratio of 10^6, which is promising for logic devices [5]. The bandgap of BP is strongly dependent on its thickness, with ~1.8 eV for monolayer, and gradually decrease to ~0.3 eV for bulk, as shown in Fig. 4(a) and (b) [15]. Therefore, few-layer BP is very suitable for optoelectronic devices with working wavelength in near-IR or mid-IR region. Photodetectors with response wavelength up to ~3 μm has already been demonstrated, which shows ultrafast response in GHz [10]. In determining the thickness of BP, the most efficient way would be using optical contrast. The optical image of 1–5 layer BP on 285 nm SiO_2/Si substrate is shown in Fig. 4(c) (a long pass filter is used here before the camera), and its corresponding white light reflection image is shown in Fig. 4(d) [28]. By using Eq. (1), the corresponding contrast spectra of BP with different thicknesses can be obtained (Fig. 4(e)). As can be seen in Fig. 4(f), the contrast increases gradually with the increase of its thickness, and the thickness of 1 and 5 layer samples are verified by AFM in the inset [28]. A relationship between the thickness of BP and its color in the optical image is further established as shown in Fig. 4(g), which is very convenient for rough determination of its thickness [64].

The final example of 2D materials discussed here is BN. Hexagonal BN (hBN) is an insulator with bandgap larger than 5 eV [6]. Because of the ultra-smooth surface as well as limited charge fluctuation, hBN has been considered as an ideal substrate for 2D materials for electronic device applications [12,65]. It has also been widely used as dielectric or tunnel barriers for heterostructures [11]. However, the hunting of hBN monolayer has been a great challenge mainly due to its zero opacity (hBN does not absorb visible light). By putting hBN on 300 nm SiO_2/Si substrate and taking advantage of the multilayer interference effect, the wavelength dependent optical contrast can be obtained as shown in Fig. 4(h) (top) [66]. However, the contrast appear positive and negative values for different wavelength, and the averaged white light contrast value could be very small (<1.5%) by integrating the whole spectra regime (it is not zero considering the non-uniform wavelength dependence of white light source). Such problems can be partially solved by using a bandpass filter before the charge-coupled device (CCD), which would select the highest contrast value in the whole spectra regime (Fig. 4(h)(bottom)) [66]. Another choice would be changing the thickness of SiO_2 layer to ~80 nm, which would increase the contrast of hBN to ~2.5% per layer, similar to that of single layer suspended graphene or graphene on transparent substrate. It is also suggested that the minimum contrast value of the hBN varies linearly with its thickness, which is ~2.5% per layer on 280 nm SiO_2/Si substrate, and therefore can be used to determine the thickness of sample very accurately, as shown in Fig. 4(i) [67]. Using the same optical contrast techniques, the thickness of other 2D materials can also be well identified, including group III metal chalcogenides: InSe [68], GaS and GaSe [29].

4. Optical image for quick and large-scale layer number determination

The above mentioned contrast spectroscopy in determination of the thickness of 2D materials rely on spectrometer to obtain the contrast spectra and adopt the contrast peak value to identify the thickness. For large scale samples, e.g., CVD grown graphene with wafer size, it would be time-consuming and challenging to obtain the contrast spectra point by point. Following, we will describe a simpler and more efficient technique that would only require an optical microscope to determine the thickness of 2D materials, namely white light contrast image technique.

The calculated contrast spectra of 1–9 layer graphene on 285 nm SiO_2/Si substrate is shown in Fig. 5(a) [69]. A CCD in a normal microscope would allow us to obtain the R, G, B values for each pixels, where a common Bayer RGB filter in CCD has B filter corresponding to 435–520 nm, G filter corresponding to 520–590 nm, and R filter corresponding to 590–720 nm [70]. Therefore, the optical images of R, G, B channels actually represent the averaged contrast values in

Please cite this article in press as: D. Bing, et al., Optical contrast for identifying the thickness of two-dimensional materials, Optics Communications (2017), http://dx.doi.org/10.1016/j.optcom.2017.06.012.

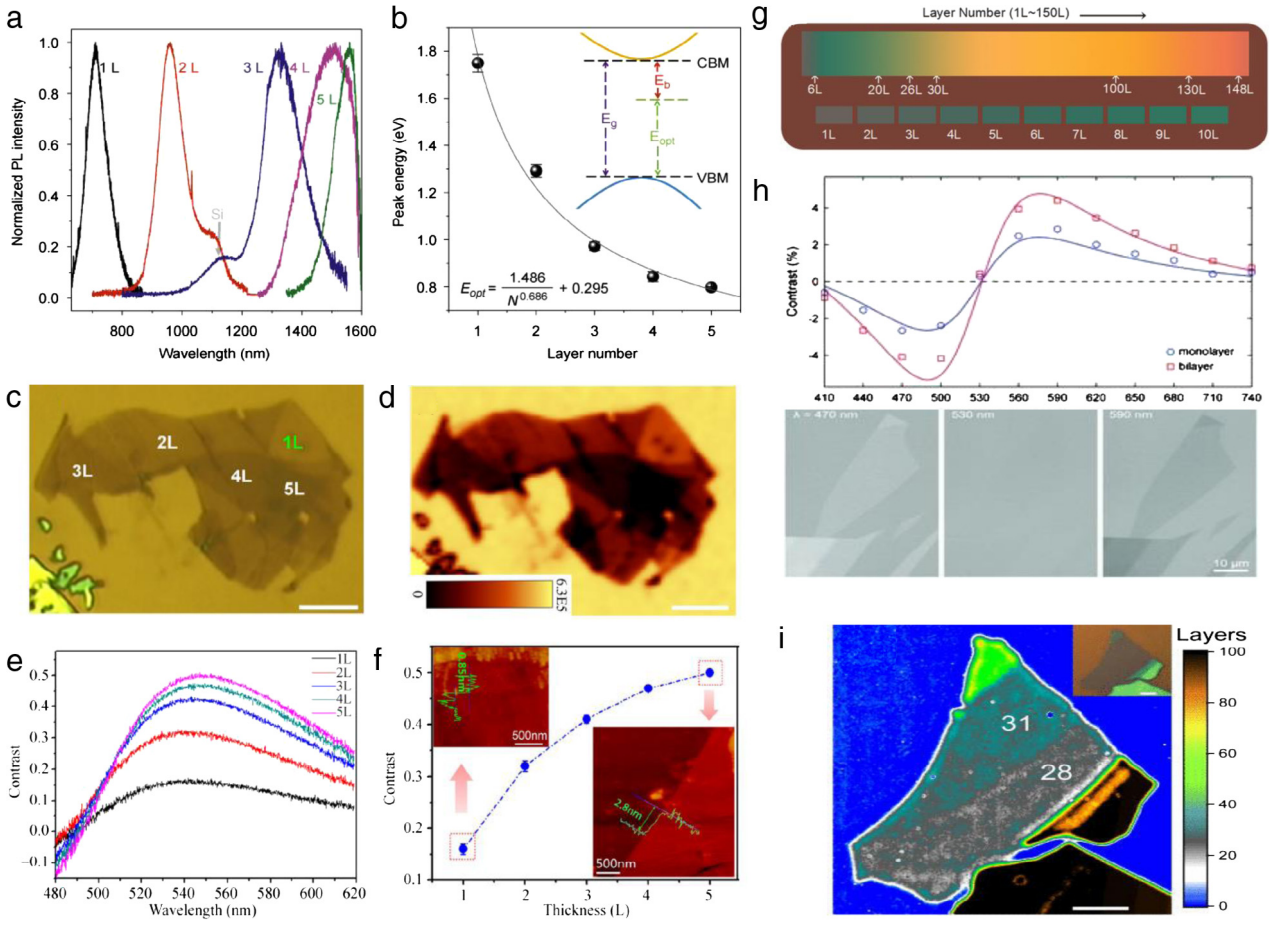

Fig. 4. Optical contrast of BP and BN. PL spectra (a) as well as emission energy (b) of BP with different thicknesses [15]. The optical image (c), white light reflection image (d), optical contrast spectra (e) as well as contrast peak values (f) of 1–5 layer BP on 285 nm SiO_2/Si substrate [28]. (g) A relationship between the thickness of BP and its color in the optical image [64]. (h) The wavelength dependent optical contrasts of hBN on 300 nm SiO_2/Si substrate (top). The optical images of hBN on 300 nm SiO_2/Si substrate with different bandpass filters (bottom) [66]. (i) Optical image of hBN with different thicknesses on a 282 nm SiO_2 substrate. The thicknesses of hBN can be precisely obtained by contrast methods [67].

their corresponding wavelength range (as shown by different colors in Fig. 5(a)). As can be seen in the RGB channel optical images of graphene layers (Fig. 5(b)), G channel image gives highest visibility of graphene on 285 nm SiO_2/Si substrate, because it covers most of the wavelength region where contrast peak locates. On the other hand, single layer graphene looks blur in R channel image and can hardly be seen in B channel image. By using $(G_{sub} - G_{sample})/G_{sub}$, where G_{sub} and G_{sample} are reflected light intensities in G channels from substrate and graphene, one would find that the theoretical calculated averaged G channel contrast values match quite well with experimental results, i.e. 0.077 for single layer graphene, and increase almost linearly up to four layers, as shown in Fig. 5(c) [69]. This value is a bit smaller than the contrast peak value (~0.095) in Fig. 1(d), but is good enough for identifying the thickness of graphene. Researchers also directly used the RGB channel values or even the total color values to determine the thickness of 2D materials [30,31], however, such value would be affected by the intensity and type of incident white light. The use of contrast in certain channel here would ensure that a quantitative normalized value is obtained and can be used to determine the thickness reliably. Such an optical image technique is universal for different 2D materials, for example, InSe [68], $NbSe_2$ [71], h-BN [72] and TaS_2 [73]. However, for different 2D materials and different substrate, the choosing of RGB channels could be much different. For example, the difference between reflection intensities of MoS_2 and substrate are higher for R channel as compared to G and B channels, both on 90 nm (Fig. 5(d)) and 300 nm (Fig. 5(e)) SiO_2/Si substrates [73]. As a result, the contrast of MoS_2 is higher for R channel and its value can be as high as ~0.125 for monolayer MoS_2 on 285 nm SiO_2/Si substrate (Fig. 5(f)) [21]. This value is even larger than G channel contrast of monolayer graphene, partially because MoS_2 is a semiconducting materials and it has larger density of states at electronic band edge, which ensures more absorption cross-sections. The advantage of this contrast image technique is that, by simple taking the optical image of 2D materials on substrate and obtaining certain RGB values at each pixel with commercial software (e.g. Matlab), the optical contrast can be easily obtained and the thickness is well identified. Moreover, such technique is ready for large scale investigation. A CVD grown single layer graphene with multilayer domains is shown in Fig. 5(g) [74]. By taking the G channel image and obtaining contrast values for each pixel, the contrast image of the whole sample can be obtained, as shown in Fig. 5(h). A histogram of the contrast values in the whole image is shown in Fig. 5(i). As can be seen, there are mainly three peaks, corresponding to contrast value of 0.091, 0.155, 0.211 and 0.259, that is 1–4 layer graphene. By integrating the whole area of each peak in Fig. 5(i), the ratio of coverage for 1–4 layers graphene can then be obtained, which is 36.46%, 52.42%, 9.01% and 2.11% respectively [74]. The above example does demonstrate that contrast image instead of contrast spectra is more suitable for large scale and low cost identification of the thickness of 2D materials, which can possibly be adopted for graphene quality control in the future.

5. Factors that affect the optical contrasts

In the above sections, we have discussed that contrast spectroscopy and imaging could be used to efficiently identify the thickness of two dimensional materials. However, there are different factors that would affect the optical contrast of 2D materials. The first issue would be the

Please cite this article in press as: D. Bing, et al., Optical contrast for identifying the thickness of two-dimensional materials, Optics Communications (2017), http://dx.doi.org/10.1016/j.optcom.2017.06.012.

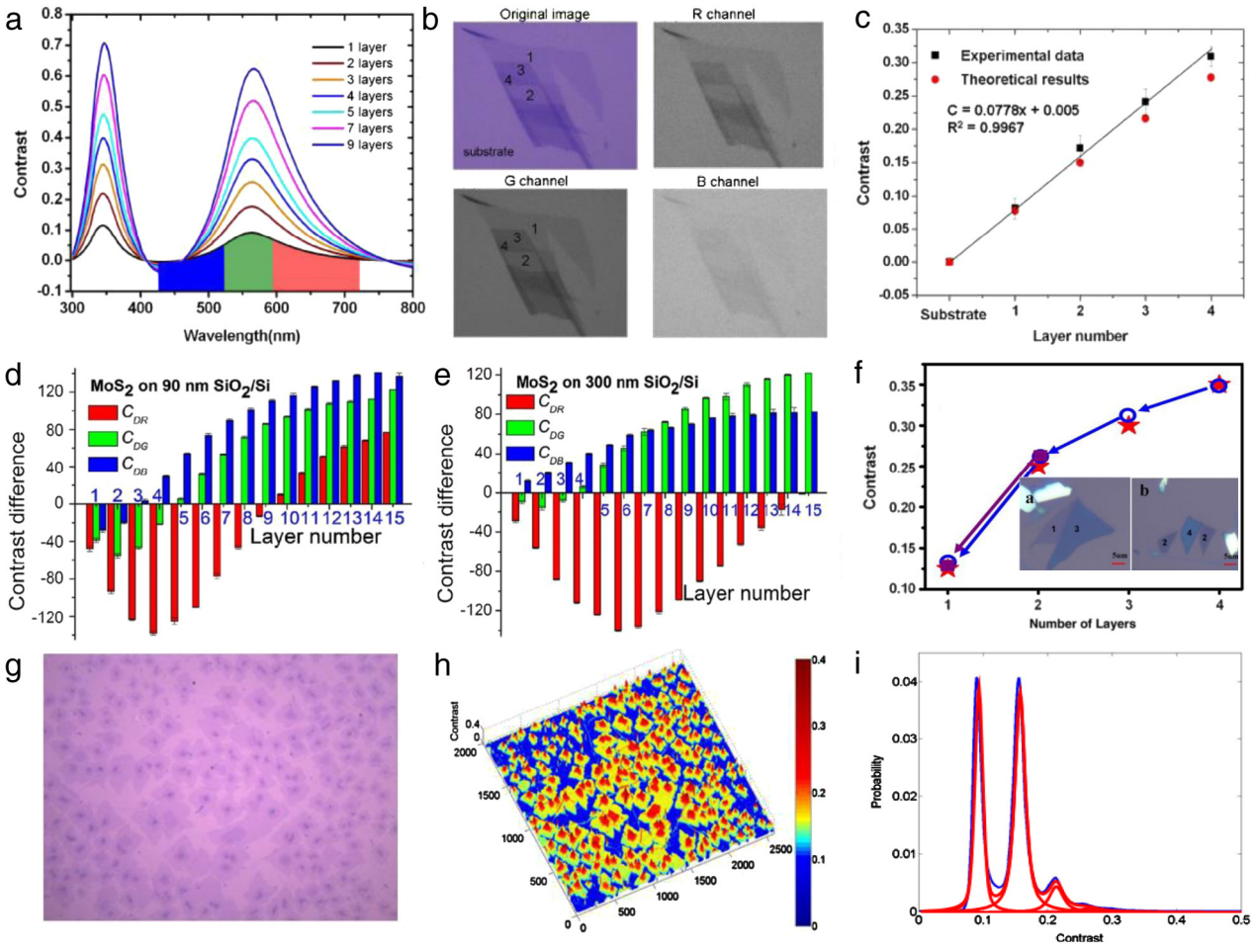

Fig. 5. Optical contrast image for quick and large-scale thickness identification. (a) Calculated contrast spectra of 1–9 layer graphene on 285 nm SiO_2/Si substrate. The wavelength regions corresponding RGB values of CCD are labeled by different colors [69]. (b) Optical image as well as RGB channel images of graphene layers on 285 nm SiO_2/Si substrate [69]. (c) Theoretical and experimental obtained G channel contrast values of 1–4 layers graphene on 285 nm SiO_2/Si substrate [69]. The difference in RGB values of MoS_2 with different thicknesses on 90 (d) and 300 (e) nm SiO_2/Si substrate [73]. (f) R channel contrast values of MoS_2 of 1–4 layers on 285 nm SiO_2/Si substrate [21]. Optical image (g), contrast image (h) as well as histogram of the contrast values (i) of a CVD grown single layer graphene with multilayer domains [74]. (For interpretation of the references to color in this figure legend, the reader is referred to the web version of this article.)

substrate, especially the thickness and refractive index of dielectric layer for the multilayer interference system [75], which have been discussed extensively in Section 3. Following, other issues that could also affect the measurement of optical contrast, including the angle of incident light, the in-plane anisotropy of some 2D materials, and also the twist angle between layers of 2D materials will be discussed.

5.1. Angle of incident light

In the above discussion, light incident is assumed to be normal to the sample and substrate, which would make the theoretical calculation much easier. However, in the real experimental microscopic configuration, white illumination light is usually focused on the sample with an objective lens with different numerical aperture (NA). A low NA lens would have most of the light with or close to normal incidence, while for a high NA lens the distribution of angles of incidence should be considered, as shown in Fig. 6(a). Larger angles of incidence would dominate if the light focused by a high NA lens, and therefore the total optical path difference would reduce. Therefore, the experimental contrast spectra of single and bilayer graphene measured under microscope with NA = 0.95 (black lines in Fig. 6(b)) do not match with those simulated by normal incidence [32]. There is a blueshift of contrast peak and also the magnitude of the peak intensity drops as compared to theoretical value with normal incidence (dash lines in Fig. 6(b)). The light that is incident on the objective may not have spatially uniform intensity, therefore, simulated results with NA = 0.63 (red lines in Fig. 6(b)) match well with the experimental data. Detailed calculations show that, with the increase of NA of objective, the wavelength as well as the magnitude of the contrast peak would gradually decrease (Fig. 6(c)). Similar results have also been shown in Fig. 6(d), where the contrast of 1–10 layers graphene have been calculated with NA = 0 and NA = 0.9 [76]. These results actually call for attentions that it should be extremely careful and a calibration should be made before using a microscope objective lens to conduct a contrast experiments. It should also be noted that although high NA could favor the spatial resolution of the optical image, it adversely affects the contrast which is important for identifying 2D materials.

In another study, the polarization of incident light was also considered, as shown in Fig. 6(e) [33]. It is found that in a TM polarization, that is, the magnetic field component is parallel to the 2D materials and electrical component is within the incident plane, the contrast value decreases with the increase of incident angle and there is a blueshift of contrast peak. However, in a TE polarization light, the contrast peak shift to lower wavelength but the magnitude is increased, which means the contrast of 2D materials at blue light region could be enhanced by using a TE polarization light with larger incident angle.

Please cite this article in press as: D. Bing, et al., Optical contrast for identifying the thickness of two-dimensional materials, Optics Communications (2017), http://dx.doi.org/10.1016/j.optcom.2017.06.012.

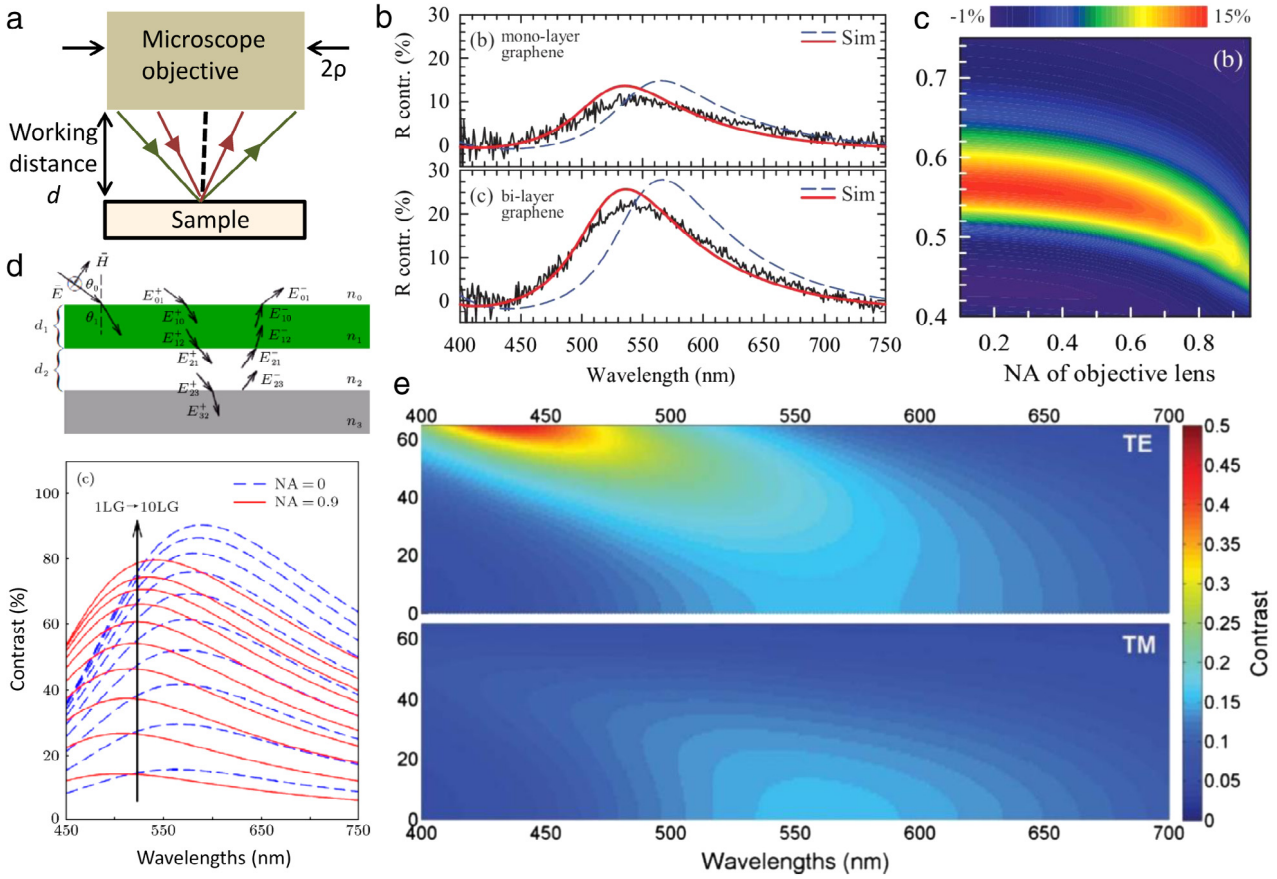

Fig. 6. The effect of incident angle on optical contrast. (a) Schematic of light incident through a high NA lens. (b) The experimental (black lines) contrast spectra of single and bilayer graphene measured under microscope with NA = 0.95, and the theoretical calculated spectra with normal incidence (dash lines) and with NA = 0.63 (red lines) [32]. (c) The calculated wavelength dependent optical contrast of graphene with different NA of objective [32]. (d) Calculated contrast spectra of 1–10 layers graphene with NA = 0 and NA = 0.9 [76]. (e) The calculated optical contrasts of graphene with different incident angles for TE and TM polarization light [33]. (For interpretation of the references to color in this figure legend, the reader is referred to the web version of this article.)

5.2. Anisotropy of materials

Some of the 2D materials have anisotropic in-plane crystal structure, such as BP [5]. The anisotropic natures include electrical, mechanical and optical properties [77–80], which are mainly related to the sp^3 nonequivalent hybridization of P atoms in plane as shown in Fig. 7(a) [28]. The optical anisotropic property would greatly facilitate BP toward functional optoelectronics, e.g. photodetector with polarization selectivity [77]. The anisotropic nature can also be probed by polarized optical contrast by rotating the sample with different angles related to the polarization direction of a analyzer in front of CCD [34]. As shown in Fig. 7(b), the optical brightness of BP changes obviously with the rotation of angles, which could be clearly seen in the RGB values in Fig. 7(c). The crystal orientation of few-layer BP can be determined by polarized Raman spectroscopy [78,81] in the polar plot of the A_g^2 mode, as shown in Fig. 7(d) and (e), where the Zigzag (ZZ) direction is along 15° and armchair (AC) direction is along 105°. Coincidently, the maximum optical contrast of the same sample is along the ZZ direction (Fig. 7(f)). This is actually corresponding to the birefringence of the BP crystal, whereas the incident polarized light can be split into s (ZZ) and p (AC) polarized brunches, which travel at different velocities [34]. The above results do inform that by simply taking the optical contrast of the BP in polarization configuration, the crystal orientation as well as other optical parameters (e.g. refractive index n and k) of the anisotropic crystals can be obtained, which would greatly facilitate the fundamental researches and devices fabrication of BP.

5.3. Twist angle dependence of the optical contrast

The electronic band structures of 2D materials can also be affected by the change of twisted angles between layers. A lot of interesting phenomena have been discovered such as tunable Van Hove Singularities (VHSs), adjustable chirality tunneling, resonant Raman scattering and changes of electronic bandgap [82–84]. All these phenomena are directly dependent on the twist angles. The tunable VHSs could actually affect the optical absorption of bilayer graphene (BLG), as shown in Fig. 8(a) [35]. For a Bernal stacked BLG, the absorption is universal in visible range and increase in the UV region due to the increase of density of states. However, if a twist angle between two layers appears, an additional absorption peak could appear due to the change of energy difference between VHSs, and the wavelength of this peak is dependent on the twist angles, that is, larger twist angle would result in additional contrast peak at lower wavelength or higher energy, as shown in Fig. 8(b) [85]. As a result, the optical contrast of twisted bilayer graphene could also be different from that of Bernal stacked BLG, where an shoulder peak appears at ~600 nm for 13.7° TBG [35]. In a CVD grown graphene sample where multilayer domains commonly observed, the TBG induced change of optical properties are even more significant. As shown in Fig. 8(c), bilayer domains with different twist angles could appear different colors on SiO_2/Si substrate, and those colors are actually coming from the difference in the optical contrast, which have enhanced contrast at different wavelength for different twisted angles [36,37]. By comparing the results with Raman and low energy electron microscopy, the angles of different colors of TBG could be determined to be ~11, 13, 15° for blue, red and yellow regions. The TBG samples with different optical absorption could also be identified by

Please cite this article in press as: D. Bing, et al., Optical contrast for identifying the thickness of two-dimensional materials, Optics Communications (2017), http://dx.doi.org/10.1016/j.optcom.2017.06.012.

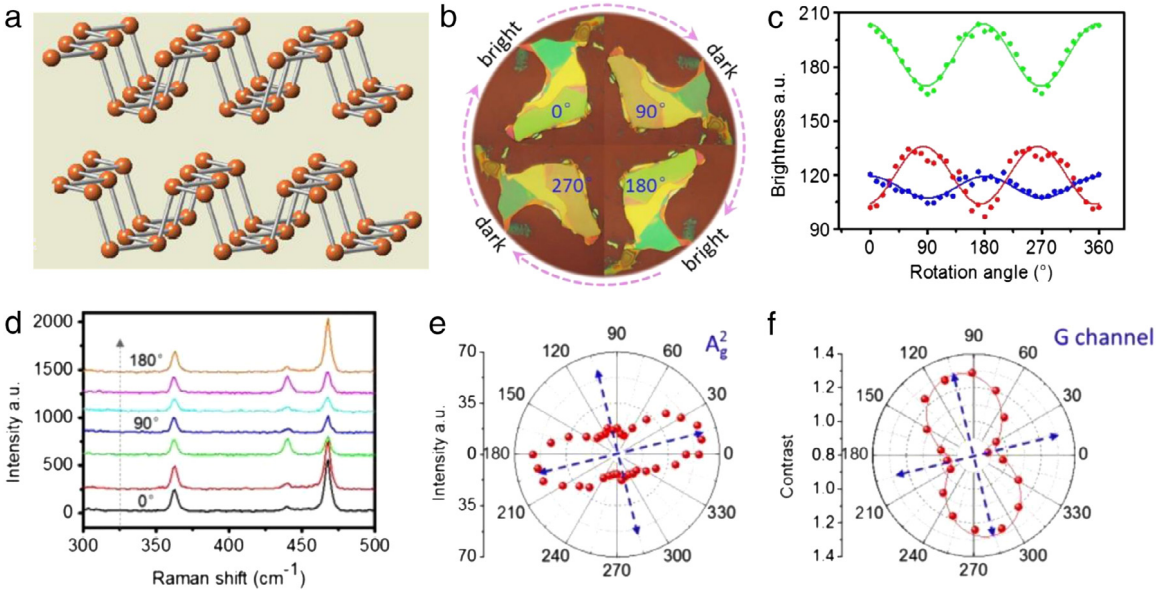

Fig. 7. The anisotropic optical contrast of BP. (a) The atomic structure of BP [28]. The optical image (b) as well as RBG values (c) of BP flakes with different rotation angles of incident light [34]. The Raman spectra (d), intensity of A_g^2 mode (e) as well as G channel contrast (f) of few-layer BP with different rotation angles of incident light [34].

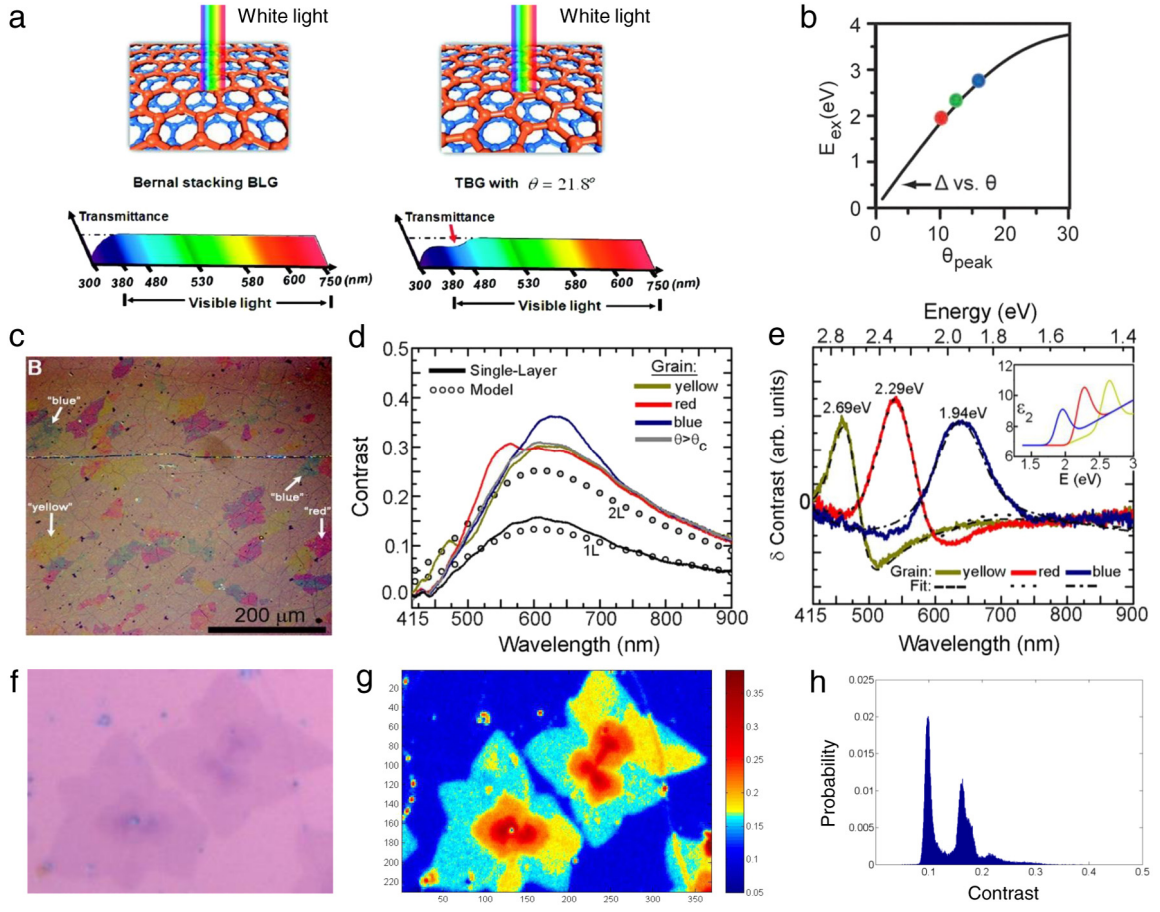

Fig. 8. Twisted angle dependence of optical contrast. (a) The schematic atomic structure as well as optical absorption of Bernal stacked and twisted bilayer graphene [35]. (b) The change of energy difference between VHSs with different twisted angles between graphene layers [85]. (c) Optical image of CVD graphene containing bilayer domains with different twist angles [85]. Contrast spectra (d) as well as contrast difference between different color regions and large angle domains (e) for multilayer domains with different colors [85]. The optical image (f), G-channel optical contrast image (g), as well as histogram of contrast values (h) of a CVD graphene with irregular shaped bilayer domains [74]. (For interpretation of the references to color in this figure legend, the reader is referred to the web version of this article.)

contrast image as shown in Fig. 8(d). By obtain the contrast difference between different color regions and large angle domains, distinct peak corresponding to the enhanced relative absorption for different regions can be obtained (Fig. 8(e)) [36]. In a CVD grown irregular shaped bilayer

Please cite this article in press as: D. Bing, et al., Optical contrast for identifying the thickness of two-dimensional materials, Optics Communications (2017), http://dx.doi.org/10.1016/j.optcom.2017.06.012.

domains (Fig. 8(f)), some of the regions have TBG with twisted angle of ~13°, which would result in the resonant Raman scattering for 514 nm excitation because this energy matches with the difference of VHSs [83]. Due to the additional optical absorption at green channel optical image, the G-channel optical contrast image of those area (yellow color regions) are a bit higher than common bilayer graphene (Fig. 8(g)) [74]. This can also be observed by the shoulder peak near the contrast peak of bilayer in histogram of the distribution of contrast values of the whole image (Fig. 8(h)) [74]. However, in the R-channel contrast image, no difference could be found for TBG and other bilayer regions, because there have no absorption difference in the red wavelength regions. The above results demonstrate that the effect of twisted angle on optical contrast could be significant for multilayer graphene and other 2D materials according to different stacking geometry.

6. Conclusion and perspective

In this review, we have introduced the basic principle of using optical contrast technique to identify the thickness of 2D materials. We also introduce the properties of different types of 2D materials, including graphene, GO, TMDs, BP and BN, and discuss the advantage of using contrast spectroscopy for thickness identification. Different methods that have been developed to enhance the optical contrast of 2D materials are also covered. We then focus on the contrast image technique that direct using the RGB values of optical image to obtain the optical contrast of 2D materials for large-scale and efficient thickness identification. Finally, different factors that could affect the optical contrast of 2D materials have been discussed, including angle of incident light (NA of the objective lens), anisotropic nature and the twist angle between layers of 2D materials. Although the optical contrast technique has been extensively developed and adopted for thickness identification of 2D materials, more efforts are expected on this area but not restricted to the following aspects: For accurate and precise thickness determination of 2D materials, different factors that would affect the contrast value should be carefully considered, including the NA of lens, the thickness of dielectric materials, the RGB range of different CCD system. Therefore, for a specific 2D material, a standard operation procedure should be developed so that the contrast technique could be widely used and the results can be compared between different research groups and also characterization centers. For newly discovered 2D materials, the using of optical contrast to identify their thicknesses should be verified by other techniques, including Raman, AFM, TEM, and also compared with the theoretical calculated contrast values. The contrast technique is very promising for large scale thickness identification of industrial samples, therefore, efforts should be put on to extend the inspection area as well as efficiency of the technique, so that it could finally be used for quality control on graphene or 2D industry. Finally, in addition to thickness identification, the optical contrast technique could also be used to achieve the optical parameter of 2D materials, including the absorption efficiency, the refractive index and other optical constants. More work should be carried out to develop the further application of optical contrast spectroscopy and image.

Acknowledgment

This work was supported by the Fundamental Research Fund of Nanjing Tech University Pujiang Institute.

References

[1] K.S. Novoselov, V.I. Falko, L. Colombo, P.R. Gellert, M.G. Schwab, K. Kim, A roadmap for graphene, Nature 490 (2012) 192–200.
[2] R. Du, W. Wang, J. Du, X. Guo, E. Liu, D. Bing, J. Bai, Photoresponse in graphene induced by defect engineering, Appl. Phys. Express 9 (2016) 115101.
[3] B. Radisavljevic, A. Radenovic, J. Brivio, V. Giacometti, A. Kis, Single-layer MoS_2 transistors, Nat. Nanotechnol. 6 (2011) 147–150.
[4] K.F. Mak, K. He, C. Lee, G.H. Lee, J. Hone, T.F. Heinz, J. Shan, Tightly bound trions in monolayer MoS_2, Nature Mater. 12 (2013) 207–211.
[5] L. Li, Y. Yu, G.J. Ye, Q. Ge, X. Ou, H. Wu, D. Feng, X.H. Chen, Y. Zhang, Black phosphorus field-effect transistors, Nat. Nanotechnol. 9 (2014) 372–377.
[6] D. Golberg, Y. Bando, Y. Huang, T. Terao, M. Mitome, C. Tang, C. Zhi, Boron nitride nanotubes and nanosheets, ACS Nano 4 (2010) 2979–2993.
[7] J. Ji, X. Song, J. Liu, Z. Yan, C. Huo, S. Zhang, M. Su, L. Liao, W. Wang, Z. Ni, Y. Hao, H. Zeng, Two-dimensional antimonene single crystals grown by van der Waals epitaxy, Nature Commun. 7 (2016) 13352.
[8] L. Tao, E. Cinquanta, D. Chiappe, C. Grazianetti, M. Fanciulli, M. Dubey, A. Molle, D. Akinwande, Silicene field-effect transistors operating at room temperature, Nat. Nanotechnol. 10 (2015) 227–231.
[9] M.E. Dávila, L. Xian, S. Cahangirov, A. Rubio, G.L. Lay, Germanene: a novel two-dimensional germanium allotrope akin to graphene and silicene, New J. Phys. 16 (2014) 095002.
[10] N. Youngblood, C. Chen, S.J. Koester, M. Li, Waveguide-integrated black phosphorus photodetector with high responsivity and low dark current, Nature Photon. 9 (2015) 247–252.
[11] F. Withers, O. Del Pozo-Zamudio, A. Mishchenko, A.P. Rooney, A. Gholinia, K. Watanabe, T. Taniguchi, S.J. Haigh, A.K. Geim, A.I. Tartakovskii, K.S. Novoselov, Light-emitting diodes by band-structure engineering in van der Waals heterostructures, Nature Mater. 14 (2015) 301–306.
[12] E. Wang, X. Lu, S. Ding, W. Yao, M. Yan, G. Wan, K. Deng, S. Wang, G. Chen, L. Ma, J. Jung, A.V. Fedorov, Y. Zhang, G. Zhang, S. Zhou, Gaps induced by inversion symmetry breaking and second-generation Dirac cones in graphene/hexagonal boron nitride, Nat. Phys. 12 (2016) 1111–1115.
[13] Y. Zhang, T.-T. Tang, C. Girit, Z. Hao, M.C. Martin, A. Zettl, M.F. Crommie, Y.R. Shen, F. Wang, Direct observation of a widely tunable bandgap in bilayer graphene, Nature 459 (2009) 820–823.
[14] K.F. Mak, C. Lee, J. Hone, J. Shan, T.F. Heinz, Atomically thin MoS_2: A new direct-gap semiconductor, Phys. Rev. Lett. 105 (2010) 136805.
[15] J. Yang, R. Xu, J. Pei, Y.W. Myint, F. Wang, Z. Wang, S. Zhang, Z. Yu, Y. Lu, Optical tuning of exciton and trion emissions in monolayer phosphorene, Light Sci. Appl. 4 (2015) e312.
[16] K.S. Kim, Y. Zhao, H. Jang, S.Y. Lee, J.M. Kim, K.S. Kim, J.-H. Ahn, P. Kim, J.-Y. Choi, B.H. Hong, Large-scale pattern growth of graphene films for stretchable transparent electrodes, Nature 457 (2009) 706–710.
[17] D. Graf, F. Molitor, K. Ensslin, C. Stampfer, A. Jungen, C. Hierold, L. Wirtz, Spatially resolved Raman spectroscopy of single- and few-layer graphene, Nano Lett. 7 (2007) 238–242.
[18] K.V. Emtsev, A. Bostwick, K. Horn, J. Jobst, G.L. Kellogg, L. Ley, J.L. McChesney, T. Ohta, S.A. Reshanov, J. Rohrl, E. Rotenberg, A.K. Schmid, D. Waldmann, H.B. Weber, T. Seyller, Towards wafer-size graphene layers by atmospheric pressure graphitization of silicon carbide, Nature Mater. 8 (2009) 203–207.
[19] E. Stolyarova, K.T. Rim, S. Ryu, J. Maultzsch, P. Kim, L.E. Brus, T.F. Heinz, M.S. Hybertsen, G.W. Flynn, High-resolution scanning tunneling microscopy imaging of mesoscopic graphene sheets on an insulating surface, Proc. Natl. Acad. Sci. 104 (2007) 9209–9212.
[20] Z. Ni, Y. Wang, T. Yu, Z. Shen, Raman spectroscopy and imaging of graphene, Nano Res. 1 (2008) 273–291.
[21] Y. Liu, H. Nan, X. Wu, W. Pan, W. Wang, J. Bai, W. Zhao, L. Sun, X. Wang, Z. Ni, Layer-by-layer thinning of MoS_2 by plasma, ACS Nano 7 (2013) 4202–4209.
[22] Z. Wu, Z. Luo, Y. Shen, W. Zhao, W. Wang, H. Nan, X. Guo, L. Sun, X. Wang, Y. You, Z. Ni, Defects as a factor limiting carrier mobility in WSe2: A spectroscopic investigation, Nano Res. 9 (2016) 3622–3631.
[23] Y. Li, Y. Rao, K.F. Mak, Y. You, S. Wang, C.R. Dean, T.F. Heinz, Probing symmetry properties of few-layer MoS_2 and h-BN by optical second-harmonic generation, Nano Lett. 13 (2013) 3329–3333.
[24] Z.H. Ni, H.M. Wang, J. Kasim, H.M. Fan, T. Yu, Y.H. Wu, Y.P. Feng, Z.X. Shen, Graphene thickness determination using reflection and contrast spectroscopy, Nano Lett. 7 (2007) 2758–2763.
[25] I. Jung, M. Pelton, R. Piner, D.A. Dikin, S. Stankovich, S. Watcharotone, M. Hausner, R.S. Ruoff, Simple approach for high-contrast optical imaging and characterization of graphene-based sheets, Nano Lett. 7 (2007) 3569–3575.
[26] H. Yang, H. Hu, Y. Wang, T. Yu, Rapid and non-destructive identification of graphene oxide thickness using white light contrast spectroscopy, Carbon 52 (2013) 528.
[27] H.-C. Kim, H. Kim, J.-U. Lee, H.-B. Lee, D.-H. Choi, J.-H. Lee, W.H. Lee, S.H. Jhang, B.H. Park, H. Cheong, S.-W. Lee, H.-J. Chung, Engineering optical and electronic properties of WS2 by varying the number of layers, ACS Nano 9 (2015) 6854–6860.
[28] W. Lu, H. Nan, J. Hong, Y. Chen, C. Zhu, Z. Liang, X. Ma, Z. Ni, C. Jin, Z. Zhang, Plasma-assisted fabrication of monolayer phosphorene and its Raman characterization, Nano Res. 7 (2014) 853–859.
[29] D.J. Late, B. Liu, H.S.S.R. Matte, C.N.R. Rao, V.P. Dravid, Rapid characterization of ultrathin layers of chalcogenides on SiO_2/Si substrates, Adv. Funct. Mater. 22 (2012) 1894–1905.
[30] H. Li, G. Lu, Z. Yin, Q. He, H. Li, Q. Zhang, H. Zhang, Optical identification of single- and few-layer MoS_2 sheets, Small 8 (2012) 682–686.
[31] L. Gao, W. Ren, F. Li, H.-M. Cheng, Total color difference for rapid and accurate identification of graphene, ACS Nano 2 (2008) 1625–1633.

Please cite this article in press as: D. Bing, et al., Optical contrast for identifying the thickness of two-dimensional materials, Optics Communications (2017), http://dx.doi.org/10.1016/j.optcom.2017.06.012.

[32] N. Saigal, A. Mukherjee, V. Sugunakar, S. Ghosh, Angle of incidence averaging in reflectance measurements with optical microscopes for studying layered two-dimensional materials, Rev. Sci. Instrum. 85 (2014) 073105.
[33] V. Yu, M. Hilke, Large contrast enhancement of graphene monolayers by angle detection, Appl. Phys. Lett. 95 (2009) 151904.
[34] N. Mao, J. Tang, L. Xie, J. Wu, B. Han, J. Lin, S. Deng, W. Ji, H. Xu, K. Liu, Optical anisotropy of black phosphorus in the visible regime, J. Am. Chem. Soc. 138 (2015) 300.
[35] Y. Wang, Z. Ni, L. Liu, Y. Liu, C. Cong, T. Yu, X. Wang, D. Shen, Z. Shen, Stacking-dependent optical conductivity of bilayer graphene, ACS Nano 4 (2010) 4074–4080.
[36] J.T. Robinson, S.W. Schmucker, C.B. Diaconescu, J.P. Long, J.C. Culbertson, T. Ohta, A.L. Friedman, T.E. Beechem, Electronic hybridization of large-area stacked graphene films, ACS Nano 7 (2013) 637–644.
[37] J. Campos-Delgado, G. Algara-Siller, C.N. Santos, U. Kaiser, J.P. Raskin, Twisted Bi-Layer graphene: microscopic rainbows, Small 9 (2013) 3247–3251.
[38] C. Casiraghi, A. Hartschuh, E. Lidorikis, H. Qian, H. Harutyunyan, T. Gokus, K.S. Novoselov, A.C. Ferrari, Rayleigh imaging of graphene and graphene layers, Nano Lett. 7 (2007) 2711–2717.
[39] B. Matteo, B. Stefano, Assessment of graphene quality by quantitative optical contrast analysis, J. Phys. D: Appl. Phys. 42 (2009) 175307.
[40] P.E. Gaskell, H.S. Skulason, C. Rodenchuk, T. Szkopek, Counting graphene layers on glass via optical reflection microscopy, Appl. Phys. Lett. 94 (2009) 143101.
[41] K. Peters, A. Tittel, N. Gayer, A. Graf, V. Paulava, U. Wurstbauer, W. Hansen, Enhancing the visibility of graphene on GaAs, Appl. Phys. Lett. 99 (2011) 191912.
[42] P. Blake, E.W. Hill, A.H.C. Neto, K.S. Novoselov, D. Jiang, R. Yang, T.J. Booth, A.K. Geim, Making graphene visible, Appl. Phys. Lett. 91 (2007) 063124.
[43] S. Akcöltekin, M.E. Kharrazi, B. Köhler, A. Lorke, M. Schleberger, Graphene on insulating crystalline substrates, Nanotechnology 20 (2009) 155601.
[44] H.S. Skulason, P.E. Gaskell, T. Szkopek, Optical reflection and transmission properties of exfoliated graphite from a graphene monolayer to several hundred graphene layers, Nanotechnology 21 (2010) 295709.
[45] R.R. Nair, P. Blake, A.N. Grigorenko, K.S. Novoselov, T.J. Booth, T. Stauber, N.M.R. Peres, A.K. Geim, Fine structure constant defines visual transparency of graphene, Science 320 (2008) 1308.
[46] X. Wang, M. Zhao, D.D. Nolte, Optical contrast and clarity of graphene on an arbitrary substrate, Appl. Phys. Lett. 95 (2009) 081102.
[47] L. Lei, B. Jingwei, Q. Yongquan, H. Yu, D. Xiangfeng, Single-layer graphene on Al_2O_3/Si substrate: better contrast and higher performance of graphene transistors, Nanotechnology 21 (2010) 015705.
[48] H. Gonçalves, L. Alves, C. Moura, M. Belsley, T. Stauber, P. Schellenberg, Enhancement of graphene visibility on transparent substrates by refractive index optimization, Opt. Express 21 (2013) 12934–12941.
[49] G. Teo, H. Wang, Y. Wu, Z. Guo, J. Zhang, Z. Ni, Z. Shen, Visibility study of graphene multilayer structures, J. Appl. Phys. 103 (2008) 124302.
[50] G. Eda, G. Fanchini, M. Chhowalla, Large-area ultrathin films of reduced graphene oxide as a transparent and flexible electronic material, Nat. Nanotechnol. 3 (2008) 270–274.
[51] H. Chang, Z. Sun, M. Saito, Q. Yuan, H. Zhang, J. Li, Z. Wang, T. Fujita, F. Ding, Z. Zheng, F. Yan, H. Wu, M. Chen, Y. Ikuhara, Regulating infrared photoresponses in reduced graphene oxide phototransistors by defect and atomic structure control, ACS Nano 7 (2013) 6310–6320.
[52] J.-M. Yun, J.-S. Yeo, J. Kim, H.-G. Jeong, D.-Y. Kim, Y.-J. Noh, S.-S. Kim, B.-C. Ku, S.-I. Na, Solution-processable reduced graphene oxide as a novel alternative to PEDOT:PSS hole transport layers for highly efficient and stable polymer solar cells, Adv. Mater. 23 (2011) 4923–4928.
[53] W. Gao, L.B. Alemany, L. Ci, P.M. Ajayan, New insights into the structure and reduction of graphite oxide, Nat. Chem. 1 (2009) 403–408.
[54] K.P. Loh, Q. Bao, G. Eda, M. Chhowalla, Graphene oxide as a chemically tunable platform for optical applications, Nat. Chem. 2 (2010) 1015–1024.
[55] J. Kim, L.J. Cote, F. Kim, J. Huang, Visualizing graphene based sheets by fluorescence quenching microscopy, J. Am. Chem. Soc. 132 (2010) 260–267.
[56] O. Lopez-Sanchez, D. Lembke, M. Kayci, A. Radenovic, A. Kis, Ultrasensitive photodetectors based on monolayer MoS_2, Nat. Nanotechnol. 8 (2013) 497–501.
[57] K.F. Mak, K. He, J. Shan, T.F. Heinz, Control of valley polarization in monolayer MoS_2 by optical helicity, Nat. Nanotechnol. 7 (2012) 494–498.
[58] H. Zeng, J. Dai, W. Yao, D. Xiao, X. Cui, Valley polarization in MoS_2 monolayers by optical pumping, Nat. Nanotechnol. 7 (2012) 490–493.
[59] A. Zafar, H. Nan, Z. Zafar, Z. Wu, J. Jiang, Y. You, Z. Ni, Probing the intrinsic optical quality of CVD grown MoS_2, Nano Res. (2016) 1–10.
[60] H. Nan, Z. Wang, W. Wang, Z. Liang, Y. Lu, Q. Chen, D. He, P. Tan, F. Miao, X. Wang, J. Wang, Z. Ni, Strong photoluminescence enhancement of MoS_2 through defect engineering and oxygen bonding, ACS Nano 8 (2014) 5738–5745.
[61] C. Lee, H. Yan, L.E. Brus, T.F. Heinz, J. Hone, S. Ryu, Anomalous lattice vibrations of single- and few-layer MoS_2, ACS Nano 4 (2010) 2695–2700.
[62] Y. Li, N. Dong, S. Zhang, K. Wang, L. Zhang, J. Wang, Optical identification of layered MoS_2 via the characteristic matrix method, Nanoscale 8 (2016) 1210–1215.
[63] A. Castellanos-Gomez, N. Agraït, G. Rubio-Bollinger, Optical identification of atomically thin dichalcogenide crystals, Appl. Phys. Lett. 96 (2010) 213116.
[64] H. Chen, W. Fei, J. Zhou, C. Miao, W. Guo, Layer identification of colorful black phosphorus, Small 13 (2017) 1602336.
[65] C.R. Dean, A.F. Young, I. Meric, C. Lee, L. Wang, S. Sorgenfrei, K. Watanabe, T. Taniguchi, P. Kim, K.L. Shepard, J. Hone, Boron nitride substrates for high-quality graphene electronics, Nat. Nanotechnol. 5 (2010) 722–726.
[66] R.V. Gorbachev, I. Riaz, R.R. Nair, R. Jalil, L. Britnell, B.D. Belle, E.W. Hill, K.S. Novoselov, K. Watanabe, T. Taniguchi, A.K. Geim, P. Blake, Hunting for monolayer boron nitride: Optical and Raman signatures, Small 7 (2011) 465–468.
[67] D. Golla, K. Chattrakun, K. Watanabe, T. Taniguchi, B.J. LeRoy, A. Sandhu, Optical thickness determination of hexagonal boron nitride flakes, Appl. Phys. Lett. 102 (2013) 161906.
[68] M. Brotons-Gisbert, J.F. Sánchez-Royo, J.P. Martínez-Pastor, Thickness identification of atomically thin InSe nanoflakes on SiO_2/Si substrates by optical contrast analysis, Appl. Surf. Sci. 354 (Part B) (2015) 453–458.
[69] W. Ying Ying, G. Ren Xi, N. Zhen Hua, H. Hui, G. Shu Peng, Y. Huan Ping, C. Chun Xiao, Y. Ting, Thickness identification of two-dimensional materials by optical imaging, Nanotechnology 23 (2012) 495713.
[70] J. Henrie, S. Kellis, S.M. Schultz, A. Hawkins, Electronic color charts for dielectric films on silicon, Opt. Express 12 (2004) 1464–1469.
[71] M.M. Benameur, B. Radisavljevic, J.S. Héron, S. Sahoo, H. Berger, A. Kis, Visibility of dichalcogenide nanolayers, Nanotechnology 22 (2011) 125706.
[72] B. Ma, P. Wang, S. Ren, C. Jia, X. Guo, Versatile optical determination of two-dimensional atomic crystal layers, Carbon 109 (2016) 384–389.
[73] H. Li, J. Wu, X. Huang, G. Lu, J. Yang, X. Lu, Q. Xiong, H. Zhang, Rapid and reliable thickness identification of two-dimensional nanosheets using optical microscopy, ACS Nano 7 (2013) 10344–10353.
[74] Y. Yu, Z. Li, W. Wang, X. Guo, J. Jiang, H. Nan, Z. Ni, Investigation of multilayer domains in large-scale CVD monolayer graphene by optical imaging, J. Semicond. 38 (2017) 033003-1.
[75] O. Wengen, Z.L. Xin, L. Qunyang, Z. Yingying, Y. Jiarui, Z. Quan-shui, Optical methods for determining thicknesses of few-layer graphene flakes, Nanotechnology 24 (2013) 505701.
[76] Han Wen-Peng, Shi Yan-Meng, Li Xiao-Li, Luo Shi-Qiang, Lu Yan, Tan Ping-Heng, The numerical-aperture-dependent optical contrast and thickness determination of ultrathin flakes of two-dimensional atomic crystals: A case of graphene multilayers, Acta Phys. Sin. 62 (2013) 110702.
[77] H. Yuan, X. Liu, F. Afshinmanesh, W. Li, G. Xu, J. Sun, B. Lian, A.G. Curto, G. Ye, Y. Hikita, Z. Shen, S.-C. Zhang, X. Chen, M. Brongersma, H.Y. Hwang, Y. Cui, Polarization-sensitive broadband photodetector using a black phosphorus vertical p–n junction, Nat. Nanotechnol. 10 (2015) 707–713.
[78] X. Wang, A.M. Jones, K.L. Seyler, V. Tran, Y. Jia, H. Zhao, H. Wang, L. Yang, X. Xu, F. Xia, Highly anisotropic and robust excitons in monolayer black phosphorus, Nat. Nanotechnol. 10 (2015) 517–521.
[79] J. Qiao, X. Kong, Z.-X. Hu, F. Yang, W. Ji, High-mobility transport anisotropy and linear dichroism in few-layer black phosphorus, Nature Commun. 5 (2014) 4475.
[80] S. Zhang, J. Yang, R. Xu, F. Wang, W. Li, M. Ghufran, et al., Extraordinary photoluminescence and strong temperature/angle-dependent Raman responses in few-layer phosphorene, ACS Nano 8 (2014) 9590.
[81] M. Buscema, D.J. Groenendijk, S.I. Blanter, G.A. Steele, H.S.J. van der Zant, A. Castellanos-Gomez, Fast and broadband photoresponse of few-layer black phosphorus field-effect transistors, Nano Lett. 14 (2014) 3347–3352.
[82] W.-Y. He, Z.-D. Chu, L. He, Chiral tunneling in a twisted graphene bilayer, Phys. Rev. Lett. 111 (2013) 066803.
[83] Z. Ni, L. Liu, Y. Wang, Z. Zheng, L.-J. Li, T. Yu, Z. Shen, G-band Raman double resonance in twisted bilayer graphene: Evidence of band splitting and folding, Phys. Rev. B 80 (2009) 125404.
[84] G. Li, A. Luican, J.M.B. Lopes dos Santos, A.H. Castro Neto, A. Reina, J. Kong, E.Y. Andrei, Observation of Van Hove singularities in twisted graphene layers, Nat. Phys. 6 (2010) 109–113.
[85] R.W. Havener, H. Zhuang, L. Brown, R.G. Hennig, J. Park, Angle-resolved Raman imaging of interlayer rotations and interactions in twisted bilayer graphene, Nano Lett. 12 (2012) 3162–3167.

Please cite this article in press as: D. Bing, et al., Optical contrast for identifying the thickness of two-dimensional materials, Optics Communications (2017), http://dx.doi.org/10.1016/j.optcom.2017.06.012.